Development 136, 2255-2264 (2009) doi:10.1242/dev.035196

Adenomatous polyposis coli regulates *Drosophila* intestinal stem cell proliferation

Wen-Chih Lee, Katherine Beebe, Lisa Sudmeier and Craig A. Micchelli*

Adult stem cells define a cellular reserve with the unique capacity to replenish differentiated cells of a tissue throughout an organism's lifetime. Previous analysis has demonstrated that the adult *Drosophila* midgut is maintained by a population of multipotent intestinal stem cells (ISCs) that resides in epithelial niches. *Adenomatous polyposis coli* (*Apc*), a tumor suppressor gene conserved in both invertebrates and vertebrates, is known to play a role in multiple developmental processes in *Drosophila*. Here, we examine the consequences of eliminating *Apc* function on adult midgut homeostasis. Our analysis shows that loss of *Apc* results in the disruption of midgut homeostasis and is associated with hyperplasia and multilayering of the midgut epithelium. A mosaic analysis of marked ISC cell lineages demonstrates that *Apc* is required specifically in ISCs to regulate proliferation, but is not required for ISC self-renewal or the specification of cell fate within the lineage. Cell autonomous activation of Wnt signaling in the ISC lineage phenocopied *Apc* loss and *Apc* mutants were suppressed in an allele-specific manner by abrogating Wnt signaling, suggesting that the effects of *Apc* are mediated in part by the Wnt pathway. Together, these data underscore the essential requirement of *Apc* in exerting regulatory control over stem cell activity, as well as the consequences that disrupting this regulation can have on tissue homeostasis.

KEY WORDS: *Drosophila*, Intestinal stem cells, Apc

INTRODUCTION

Many adult tissues require the activity of tissue-specific stem cell populations to maintain homeostasis throughout the course of an organism's lifetime. The dual characteristics of self-renewal and multipotency make stem cells ideally suited for this central role. Adult stem cells reside in specialized microenvironments called niches, which regulate stem cell behavior at baseline homeostasis and dynamically respond to changing environmental stimuli by modulating lineage output (reviewed by Jones and Wagers, 2008). Tight control of stem cell proliferation is essential to ensure that homeostatic balance is maintained; disruption of stem cell proliferation can lead to homeostatic imbalance, compromised wound healing, and disease. However, little is currently known about the factors that constrain stem cell proliferation.

The precise location and cellular architecture of the adult stem cell niche has been defined with high resolution in only a small number of tissues (reviewed by Morrison and Spradling, 2008). The ability to identify, manipulate and mark individual stem cell lineages has made *Drosophila* an excellent model system with which to dissect stem cell regulation. For example, the adult *Drosophila* midgut contains approximately 2000 intestinal stem cells (ISCs) distributed along the anteroposterior (AP) axis of the organ (Fig. 1A,B) (Micchelli and Perrimon, 2006; Ohlstein and Spradling, 2006). ISCs have a pyramidal morphology and are located in an epithelial niche distant from the midgut lumen, adjacent to the basement membrane and the visceral musculature surrounding the midgut. ISCs are multipotent and give rise to a lineage that consists of two types of differentiated daughters, the enteroendocrine (ee) cells and the enterocytes (ECs), which together form a cellular monolayer lining the length of the adult midgut.

Department of Developmental Biology, Washington University School of Medicine, 660 South Euclid Avenue, St Louis, MO 63110, USA.

*Author for correspondence (e-mail: micchelli@wustl.edu)

Accepted 28 April 2009

Adenomatous polyposis coli (*Apc*) encodes an evolutionarily conserved protein, which was first identified by positional cloning as one of the genes commonly deleted in the hereditary colon cancer syndrome familial adenomatous polyposis (FAP) (Groden et al., 1991; Kinzler et al., 1991). Mutations in both copies of *Apc* are also detected in many spontaneous colorectal adenomas (Miyoshi et al., 1992; Powell et al., 1992; Ichii et al., 1992). As the majority of *Apc* mutations are loss of function, *Apc* is thought to function as a tumor suppressor gene. Early insight into the molecular function of *Apc* came from the identification of β-catenin, a Wnt pathway effector, as a binding partner for Apc (Su et al., 1993; Rubinfeld et al., 1997). The requirement for *Apc* in the Wnt signaling pathway is now well characterized and current models suggest that Apc together with Axin, Glycogen Synthase Kinase 3 and Casein Kinase 1 comprise a multiprotein β-catenin destruction complex. In the absence of Wnt ligands, the destruction complex phosphorylates β-catenin, targeting it for proteasomal degradation.

The *Drosophila* genome, like that of both mouse and human, contains two Apc family members, *Apc1* (also known as *Apc* – FlyBase) and *Apc2* (Hayashi et al., 1997; Ahmed et al., 1998; McCartney et al., 1999; Hamada et al., 1999a). Previous analysis in *Drosophila* has implicated *Apc* in a number of developmental processes, including cell survival, cell fate specification and proliferation. Yet, the role of *Apc* in maintaining adult *Drosophila* midgut homeostasis has not been examined. In this study, we investigate the consequences of eliminating *Apc* function on adult midgut homeostasis and ISC behavior.

MATERIALS AND METHODS

Drosophila strains and culture

$Apc2^{C9}$/TM6 Tb, Hu (*$Apc2^{C9}$* is a temperature-sensitive allele with a permissive temperature of 18°C and non-permissive temperature of 27°C; gift from B. McCartney, Carnegie Mellon University, Pittsburgh, PA, USA). *w; FRT^{82B} $Apc2^{g10}$, $Apc1^{Q8}$/TM6C* (*$Apc2^{g10}$* is null for Armadillo degradation but retains the ability to promote Wnt signaling in the eye; *$Apc1^{Q8}$* is a null allele; gift from B. McCartney). *w; FRT^{82B} $Apc2^{33}$, $Apc1^{Q8}$/TM6C* (*$Apc2^{33}$* is a strong hypomorph resulting from a deletion; gift from Y. Ahmed, Dartmouth

College, Hanover, NH, USA). *w; FRT^{82B} Axin^{s044230}/TM3 Sb* (*Axin^{s044230}* is a loss-of-function allele; gift from Y. Ahmed). *y, w,UAS-GFP, hsflp; tubGal4, FRT^{82B}, tubGal80/TM6B* (gift from N. Perrimon, Harvard Medical School, Boston, MA, USA). *y, w; esgGal4/Cyo* (gift from S. Hayashi, RIKEN, Kobe, Japan). *w, UAS-N^{RNAi}. UAS-GFP*. *y, w*; *esg^{K606}/Cyo* (*esg-lacZ*). *w; FRT^{82B} hsπM* (this stock was used as a wild-type control in the mosaic analysis performed in this study). *y, w, UAS-arm^{S10}* (activated arm). *y, w; UAS-pan.dTCFΔN4* (dominant-negative allele). Unless indicated, all strains were obtained from the Bloomington Stock Center. Crosses were cultured on standard dextrose media and were transferred to fresh food augmented with yeast paste every 1-2 days during the experimental period. Crosses were reared at 18, 25, or 29°C, in passively illuminated and humidified incubators. In this study, only adult female flies of the following genotypes were analyzed.

Figure 2:
+ / w; esg^{K606} /+; FRT^{82B} Apc2^{g10}, Apc1^{Q8} / Apc2^{C9}.
+ / w; FRT^{82B} Apc2^{g10}, Apc1^{Q8} / Apc2^{C9}.

Figures 3, 4 and S2:
y, w, hsFLP, UAS-GFP / w; +; FRT^{82B} hsπM / tubGal4, FRT^{82B} tubGal80.
y, w, hsFLP, UAS-GFP / w; +; FRT^{82B} Apc2^{g10}, Apc1^{Q8} / tubGal4, FRT^{82B} tubGal80.

Figure 5:
y, w, hsFLP, UAS-GFP / w; esg ^{K606} /+; FRT^{82B} hsπM / tubGal4, FRT^{82B} tubGal80.
y, w, hsFLP, UAS-GFP / w; esg ^{K606} /+; FRT^{82B} Apc2^{g10}, Apc1^{Q8} / tubGal4, FRT^{82B} tubGal80.
y, w, hsFLP, UAS-GFP / w; +; FRT^{82B} Apc2^{g10}, Apc1^{Q8} / tubGal4, FRT^{82B} tubGal80.

Figures 6, S3 and S4:
y, w, hsFLP, UAS-GFP / w, UAS-N^{RNAi}; +; FRT^{82B} hsπM / tubGal4, FRT^{82B} tubGal80.
y, w, hsFLP, UAS-GFP / w, UAS-N^{RNAi}; +; FRT^{82B} Apc2^{g10}, Apc1^{Q8} / tubGal4, FRT^{82B} tubGal80.
y, w, hsFLP, UAS-GFP / w, UAS-N^{RNAi}; esg ^{K606} /+; FRT^{82B} hsπM / tubGal4, FRT^{82B} tubGal80.
y, w, hsFLP, UAS-GFP / w, UAS-N^{RNAi}; esg^{K606} /+; FRT^{82B} Apc2^{g10}, Apc1^{Q8} / tubGal4, FRT^{82B} tubGal80.

Figures 7 and S5:
y, w, hsFLP, UAS-GFP / w; +; FRT^{82B} hsπM / tubGal4, FRT^{82B} tubGal80.
y, w, hsFLP, UAS-GFP / w; UAS-pan.dTCFΔN4 / +; FRT^{82B} hsπM / tubGal4, FRT^{82B} tubGal80.
y, w, hsFLP, UAS-GFP / w; +; FRT^{82B} Axin^{s044230} / tubGal4, FRT^{82B} tubGal80.
y, w, hsFLP, UAS-GFP / w; UAS-pan.dTCFΔN4 /+; FRT^{82B} Axin^{s044230} / tubGal4, FRT^{82B} tubGal80.
y, w, hsFLP, UAS-GFP / w; +; FRT^{82B} Apc2^{33}, Apc1^{Q8} / tubGal4, FRT^{82B} tubGal80.
y, w, hsFLP, UAS-GFP / w; UAS-pan.dTCFΔN4 /+; FRT^{82B} Apc2^{33}, Apc1^{Q8} / tubGal4, FRT^{82B} tubGal80.
y, w, hsFLP, UAS-GFP / w; +; FRT^{82B} Apc2^{g10}, Apc1^{Q8} / tubGal4, FRT^{82B} tubGal80.
y, w, hsFLP, UAS-GFP / w; UAS-pan.dTCFΔN4 / +; FRT^{82B} Apc2^{g10}, Apc1^{Q8} / tubGal4, FRT^{82B} tubGal80.
y, w, hsFLP, UAS-GFP / y, w, UAS-arm^{S10}; +; FRT^{82B} hsπM / tubGal4, FRT^{82B} tubGal80.

Mosaic analysis
The MARCM system was used to generate marked ISC lineages or 'clones'. MARCM was used to produce both marked wild-type and mutant lineages; in addition, all manipulations involving the misexpression of UAS transgenes were also performed using the MARCM system to ensure that only ISC lineages were analyzed. To induce clones, experimental animals were subjected to a 37°C heat pulse for 35-45 minutes within the first week of adulthood. Induction protocols varied from one to three heat pulses within a 24-hour period, depending on the desired rate of mitotic recombination.

Temperature shift experiments
Crosses were established and cultured at 18°C until adulthood. F1 progeny were divided into two equal pools; controls were cultured at 18°C and the experimental group was shifted to 29°C for 10 days. BrdU was administered ad libitum in *Drosophila* food media (200 μl of 6 mg/ml BrdU in 20% sucrose per vial) for the 24-hour period immediately preceding the 10-day time point.

Histology
Adult flies were dissected in 1×PBS (Sigma, USA). The gastrointestinal tract was removed and fixed in a final solution of 0.5×PBS (Sigma, USA) and 4% electron microscopy grade formaldehyde (Polysciences, USA) for a minimum of 30 minutes. Samples were washed in 1×PBS with 0.1% Triton X-100 (PBST) for 2 hours and then incubated with primary antibodies overnight. Samples were washed in PBST for 2 hours and then incubated with secondary antibodies for 3 hours. Finally, samples were washed in PBST overnight. Mounting media containing DAPI (Vectashield, USA) was added and samples were allowed to clear for 1 hour prior to mounting. All steps were completed at 4°C, with no mechanical agitation.

Antisera
Primary antibodies
Chicken anti-GFP (Abcam, USA) used at a dilution of 1:10,000; rabbit anti-β-Gal (Cappel, USA), 1:2000; mouse anti-Pros (Developmental Studies Hybridoma Bank; DSHB), 1:100; mouse anti-Dl (DSHB), 1:10; mouse anti-BrdU (Becton Dickinson, USA), 1:100; rabbit anti-Pdm1 [gift of W. Chia (Yeo et al., 1995)], 1:1000; rabbit anti-Tachykinin [gift of D. Nässel (Siviter et al., 2000)], 1:1000.

Secondary antibodies
Goat anti-chicken Alexa 488 (Molecular Probes, USA) used at a dilution of 1:2000; goat anti-mouse Alexa 568 (Molecular Probes, USA), 1:2000; goat anti-mouse Alexa 633 (Molecular Probes, USA), 1:2000; goat anti-rabbit Alexa 568 (Molecular Probes, USA), 1:2000.

Dyes and mounting media
Alexa 594-conjugated Phalloidin (Molecular Probes, USA) diluted 1:500; Vectashield+DAPI mounting media (Vector, USA).

Microscopy and imaging
Samples were examined on a Leica DM5000 upright fluorescent microscope. Confocal images were collected using a Leica TCS SP5 confocal microscope system. Images were processed for brightness and contrast, and assembled in Photoshop CS (Adobe, USA).

Cell counts, measurements and statistical analysis
In the temperature-shift analyses, entire midguts were scored. BrdU^{+} *esg-lacZ*$^{+}$ positive pairs of cells were scored as a single event; clusters of three cells were scored as two events. In those TS experiments lacking *esg-lacZ* only small BrdU^{+} clusters were scored (Fig. 2D). Midgut area was determined by first acquiring digital images of the posterior midgut on a compound microscope; Leica application suite (LAS) software was then used to determine the area of the posterior region. Next, the maximal number of nuclear layers and maximal epithelial height was determined based on confocal micrographs taken from the same posterior midguts. Only those regions of the epithelium from the outer face of posterior midgut, which has a larger circumference, were analyzed to minimize secondary distortion of the epithelium due to the coiled morphology of the midgut (Fig. 3E,F). In our mosaic analysis, the number of cells per clone was scored in either anterior and/or posterior midgut frames 5 days following induction (Fig. 4A; see also Fig. S1 in the supplementary material; Fig. 4D,F; Fig. 6G). Data from the anterior and posterior midgut are combined in Fig. 4D, but separated by region in Fig. 4F. Unless indicated, counts were collected from posterior frames. Clones within selected frames were defined as clusters of contiguous cells, as assessed at 40× magnification on compound or confocal microscopes. For a clone to be scored it had to lie completely in the field of view; clones that partially wrapped around the 'edge' of the midgut sample were excluded from the analysis to minimize counting inaccuracy. To determine the number of dividing cells per frame, GFP^{+} pHH3^{+} cells were counted from the middle frame of the posterior midgut 5 days after heat-shock induction (Fig. 4E). To assay ISC self-renewal, the number of clones

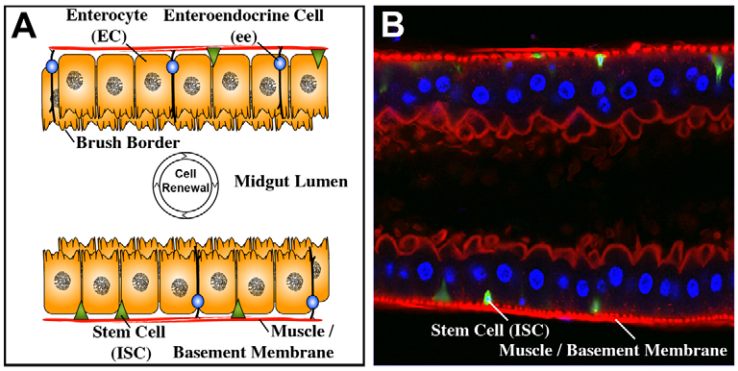

Fig. 1. The adult *Drosophila* midgut is maintained by a population of multipotent intestinal stem cells (ISCs). (**A**) Diagram of the adult midgut in cross section. ISCs (green) occupy a basal position in a niche adjacent to the basement membrane and the visceral muscle (red). ISCs give rise to two types of differentiated daughters, enteroendocrine (ee) cells (blue) and enterocytes (ECs; orange). (**B**) A cross section of the adult midgut showing ISCs marked by *esgGal4, UAS-GFP* (green). ECs have large polyploid nuclei (blue, DAPI) and form a polarized cellular monolayer with an actin-rich (red, phalloidin) brush border on their luminal surface; ee cells are not marked.

per entire midgut was scored 5 and 10 days following heat-shock induction (Fig. 4G). Mitotic index was calculated by dividing the number of pHH3$^+$ *pros*$^-$ small nuclei by the total number of *pros*$^-$ small nuclei from marked lineages in posterior midgut frames 5 days following induction (Fig. 6H; see also Fig. S4 in the supplementary material). All *t*-tests were performed using Prism (GraphPad Software, USA).

RESULTS

Apc regulates adult midgut homeostasis

Previous studies of *Apc* have demonstrated that functional redundancy exists between *Apc1* and *Apc2* in a number of *Drosophila* tissues, including the embryonic epidermis, the wing and eye imaginal discs, and the larval brain (Ahmed et al., 2002; Akong et al., 2002a; Akong et al., 2002b; McCartney et al., 2006). We therefore reasoned that simultaneous reduction of both *Apc1* and *Apc2* would be a direct means by which to initially assess the requirement for *Apc* in the adult midgut. To globally reduce *Apc* function in a conditional manner, we used a temperature-sensitive allelic combination and measured the extent of 5-bromo-2-deoxyuridine (BrdU) incorporation in the adult midgut (Fig. 2A-D). Here, we employed three well-characterized alleles of *Apc* to establish the temperature-sensitive genotype $Apc2^{g10}$, $Apc1^{Q8}/Apc2^{C9}$ [subsequently referred to as Apc^{TS} (Ahmed et al., 1998; McCartney et al., 2006)]. Unshifted control animals grown at the permissive temperature were compared with experimental animals shifted to the non-permissive temperature for 10 days during adulthood. In these experiments, we observed an increase in the number of BrdU$^+$ cells in experimental samples that often appeared as clusters of two to three small cells (Fig. 2A-C). Previous analysis has demonstrated that the transcriptional repressor encoded by *escargot* (*esg*) can be used to identify ISCs and their nascent daughters, called enteroblasts (EBs) (Fig. 2A,B) (Micchelli and Perrimon, 2006). To quantify the Apc^{TS} phenotype, we counted the number of small BrdU$^+$ clusters in the midgut following a 24-hour BrdU pulse that immediately preceded the 10-day time point (BrdU administered ad libitum in food media). Global reduction in the levels of *Apc1* and *Apc2* resulted in a significant increase in the number of BrdU$^+$ small cell clusters (Fig. 2D; n=11). This analysis suggested that *Apc* is necessary for the maintenance of midgut homeostasis in the adult.

Apc is required in ISC lineages to maintain homeostasis

Although the TS analysis suggested a role for *Apc* in regulating midgut homeostasis, it did not directly establish a requirement for *Apc* in the midgut. To test the requirement for *Apc* specifically in the midgut, we next conducted a mosaic analysis of *Apc* double mutants ($Apc2^{g10}$, $Apc1^{Q8}$; subsequently referred to as *Apc* clones, except where indicated). Positively marked ISC lineages lacking *Apc* function were generated in the adult using the MARCM system (Lee and Luo, 1999) and identified on the basis of GFP expression. At 20 days after induction, midguts containing *Apc* clones were associated with gross anatomical changes, including midgut hyperplasia and multilayered cellular masses that distorted the luminal surface of the midgut (Fig. 3A-D). Plotting the maximal number of nuclear layers as a function of midgut area revealed an inverse correlation in *Apc* mosaics and an increase in each parameter compared with wild type (Fig. 3E; wild type, n=11; *Apc*, n=12). At 20 days after induction, it was often difficult to unambiguously identify individual marked *Apc* mutant lineages because of the changes in overall midgut morphology. However,

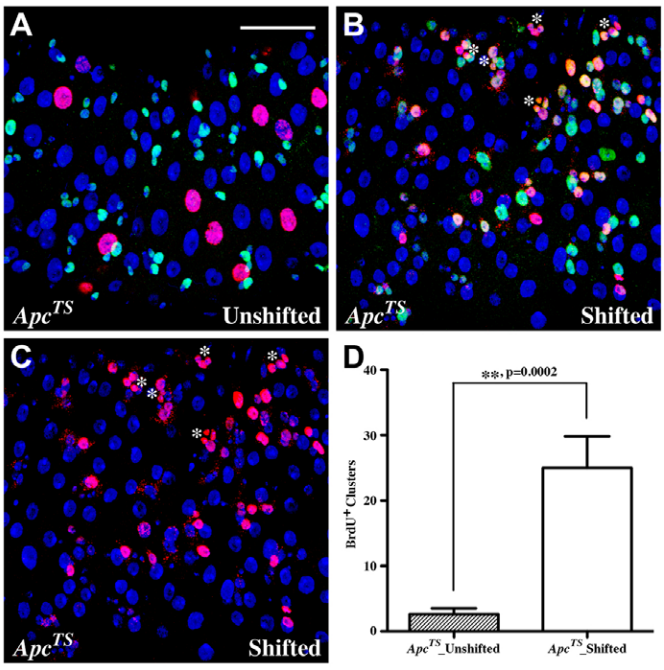

Fig. 2. *Apc* is required to maintain adult midgut homeostasis. (**A-D**) Global reduction of *Apc* family genes leads to an increase in BrdU incorporation in *esg-lacZ* cells (anti-BrdU, red; anti-βgal, green; DAPI, blue). Superficial views of midgut. (A) Apc^{TS} unshifted. Note that large polyploid EC nuclei incorporate BrdU. (B,C) Apc^{TS} shifted. Asterisks indicate *esg*$^+$ BrdU$^+$ cells. (D) Quantitation of BrdU$^+$ cells (unshifted, n=11; shifted, n=11). Error bars denote s.e.m. **P=0.0002. Scale bar: 50 μm.

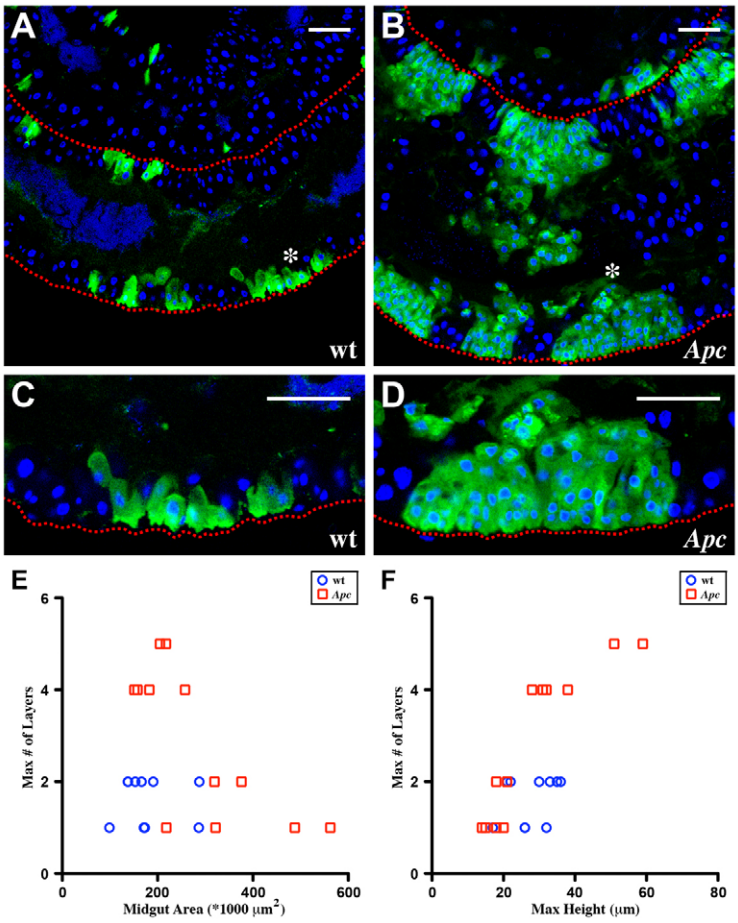

Fig. 3. Loss of *Apc* in the midgut leads to hyperplasia and multilayering. (**A-D**) The MARCM system was used to positively identify ISC lineages with GFP 20 days after induction (anti-GFP, green; DAPI, blue). Midgut viewed in cross section; dashed red line indicates midgut outline. (A) Wild-type ISC lineages. Marked cells define a single cellular layer. (B) ISC lineages lacking *Apc*. Loss of *Apc* leads to midgut hyperplasia and extensive multilayering. (C) High magnification view of A. Frame corresponds to the region on the outer face of the midgut indicated by the asterisk (A). (D) High magnification view of B. Frame corresponds to the region on the outer face of the midgut indicated by the asterisk (B). (**E**) Maximal number of midgut layers plotted as a function of midgut area in wild-type and *Apc* mosaic midguts. Note the multilayering and increased area in *Apc* mosaic midguts. (**F**) Maximal number of midgut layers plotted as a function of maximal epithelial height in wild-type and *Apc* mosaic midguts. Scale bars: 50 μm.

by plotting the maximal number of nuclear layers as a function of maximal epithelial height, it was evident that up to five layers could be detected in mosaic *Apc* midguts (Fig. 3F; wild type, n=11; *Apc*, n=12). Finally, in those cases in which individual clones could be definitively identified, *Apc* mutant lineages were found to produce multilayered masses more frequently than were wild type (*Apc*, 31.5%, n=181; wild type, 1.3%, n=227).

The analysis of *Apc* clones was extended to determine the number of labeled cells in individual ISC lineages. As we observed little or no distortion of the midgut due to multilayering at early time points, a 5-day post-induction time point was selected to quantify the number of cells per ISC clone. Cell counts were performed by scoring clones at two defined regions within each midgut analyzed (Fig. 4A; see Materials and methods and Fig. S1 in the supplementary material for experimental criteria). Mosaic analysis revealed a significant increase in the number of cells per clone in *Apc* lineages compared with in marked wild-type controls (Fig. 4B-D; n=76). This increase in clone size suggested that *Apc* loss leads to an increase in proliferation. Consistently, we observed that *Apc* mutant lineages were associated with a significant increase in the number of phospho-histone H3 positive (pHH3$^+$) cells when compared with wild-type cell lineages (Fig. 4E; wild type, n=18; *Apc*, n=17).

An analysis of *Apc* clone size along the AP axis of the gastrointestinal tract was performed to determine whether the requirement for *Apc* was dependent on midgut region. This analysis revealed a significant increase in *Apc* clone size in both the anterior and posterior midgut compared with in wild-type controls (Fig. 4F). Although the trend towards increased clone sizes in ISCs lacking *Apc* was observed throughout the midgut, the average size of *Apc* clones was found to be greater in the posterior. Taken together, our mosaic analysis demonstrates that *Apc* is required in the ISC cell lineage throughout the midgut to maintain homeostasis.

Apc loss does not affect ISC self-renewal

One possible explanation for the hyperplasia associated with *Apc* loss is that *Apc* affects ISC self-renewal. Early studies of *Drosophila* germ line stem cells employed a lineage-tracing assay to measure stem cell self-renewal (Margois and Spradling, 1995). A pulse/chase experiment was used to determine the number of marked stem cell lineages retained in the tissue at defined intervals following induction. To determine whether *Apc* loss affected ISC self-renewal in the midgut, we generated labeled ISCs and counted the number of marked ISC lineages per midgut at 5 and 10 days after induction. When the number of ISC lineages per gut lacking *Apc* was compared with wild type, no significant differences were detected (Fig. 4G). These data show that *Apc* loss does not detectably affect the fidelity of ISC self-renewal.

ISCs lacking *Apc* generate the differentiated cells of the lineage

A second possible explanation for the hyperplasia associated with *Apc* loss is that *Apc* is required for differentiation in the ISC lineage. Inspection of *Apc* clone morphology initially suggested that cell fate in the lineage was correctly specified. To more rigorously analyze cell fate in *Apc* lineages, we examined a panel of molecular markers to label distinct cell types in the ISC lineage. The transcriptional

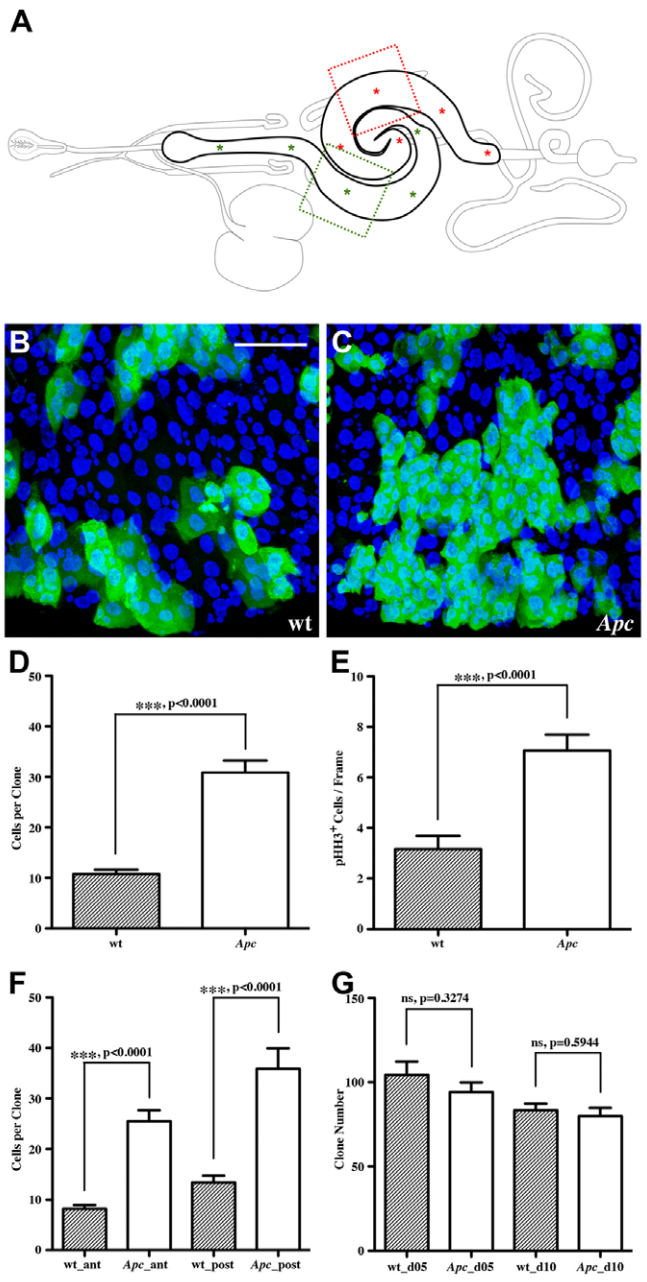

Fig. 4. Loss of *Apc* in ISCs leads to an increase in clone size. (**A**) Diagram of the adult *Drosophila* gastrointestinal tract (see Miller, 1950); midgut in heavy black outline. Data were collected from two morphologically defined regions: one in the middle of the anterior midgut (green frame) and one in the middle of the posterior midgut (red frame). (**B-G**) The MARCM system was used to positively identify ISC lineages with GFP (anti-GFP, green; DAPI, blue). (B) Wild-type ISC lineages in posterior midgut 5 days after induction, superficial view. (C) ISC lineages lacking *Apc* in posterior midgut 5 days after induction, superficial view. (D) *Apc* loss leads to an increase in the number of cells per clone (wild type, *n*=76; *Apc*, *n*=76). (E) Mosaic midguts lacking *Apc* display an increase in the number of pHH3$^+$ cells (wild type, *n*=18; *Apc*, *n*=17). (F) Analysis of *Apc* clones along the anteroposterior axis of the midgut. Compared with wild type, *Apc* clones are larger in both the anterior (wild type, *n*=38; *Apc*, *n*=37) and posterior (wild type, *n*=38; *Apc*, *n*=39) regions. (G) Self-renewal is not detectably altered in ISCs lacking *Apc* at 5 days (wild type, *n*=6; *Apc*, *n*=6) or 10 days (wild type, *n*=8; *Apc*, *n*=9) after induction. Error bars denote s.e.m. Scale bar: 50 μm.

repressor encoded by *esg* is expressed in ISCs and their undifferentiated EB daughters, but *esg* is not expressed in either of the two differentiated cell types of the midgut, the ee cells or the ECs (Fig. 5A) (Micchelli and Perrimon, 2006). Examination of *esg-lacZ* expression in *Apc* clones revealed the presence of both *esg*$^+$ and *esg*$^-$ cell populations (Fig. 5B). Similarly, elevated levels of Delta (Dl), which marks a subset of ISCs (Ohlstein and Spradling, 2007), were also detected in *Apc* clones (Fig. 5C). We note that in some instances levels of Dl appeared to be higher in certain ISC/EB pairs (Fig. 5C; see also Fig. S2B in the supplementary material). Thus, undifferentiated cells of the ISC lineage can be detected in the absence of *Apc*.

The presence of *esg*$^-$ cell populations in *Apc* lineages suggested that ee cell and EC fates had been specified in the absence of *Apc*. To test this directly, we examined *Apc* lineages for the presence of ee cells and ECs using molecular markers. To determine whether ee cell fate is specified in lineages lacking *Apc*, we examined the expression of Prospero (Pros), a marker of the ee cell population (Micchelli and Perrimon, 2006; Ohlstein and Spradling, 2006). The presence of Pros$^+$ cells was detected in *Apc* clones (Fig. 5D), as observed in wild-type cell lineages (Micchelli and Perrimon, 2006; Ohlstein and Spradling, 2006). Similarly, examination of Tachykinin (Tk) expression, which marks a specific subset of ee cells (Ohlstein and Spradling, 2006), demonstrated that *Apc* is not necessary for this ee cell subtype (Fig. 5E). Finally, differentiated ECs are distinguished by their large, polyploid nuclei (Micchelli and Perrimon, 2006; Ohlstein and Spradling, 2006), and by the expression of Pdm1 (Nubbin – FlyBase). Inspection of *Apc* clones revealed the presence of large Pdm1$^+$ nuclei within mutant lineages (Fig. 5F). Taken together, this analysis demonstrates that ISCs lacking *Apc* are capable of producing both ee cell and EC fates.

Apc is required in ISCs to regulate proliferation

Our experiments show that a reduction or loss of *Apc* leads to ISC lineages of increased size, as well as an increase in the number of both S-phase and M-phase markers. Over time, this leads to hyperplasia and multilayering of the midgut. Yet, no alteration in ISC self-renewal or cell fate specification was detected using lineage-tracing analysis. Collectively, these findings raised the possibility that *Apc* is required specifically in ISCs to regulate proliferation. Previous analyses demonstrated that targeted knockdown of Notch (N) in ISCs leads to an expansion of *esg*$^+$ cell number in the midgut (Micchelli and Perrimon, 2006). Similarly, the generation of ISC lineages completely lacking *N* function leads to an expanded clonal population of undifferentiated cells (Ohlstein and Spradling, 2006). Thus, reduction of N function generates a population of ectopic cells that exhibit the characteristics of midgut ISCs.

If *Apc* functions specifically in ISCs to limit proliferation, then we predict that the loss of *Apc* should enhance the severity of the N loss-of-function phenotype. To directly test this possibility, we compared the number of cells per clone generated by ISCs lacking N with the number generated by ISCs lacking both N and *Apc*. Using the MARCM system, we created *Apc* mosaics that simultaneously expressed a N^{RNAi} transgene (Presente et al., 2002) (N^{RNAi}, $Apc2^{g10}$, $Apc1^{Q8}$; subsequently referred to as N^{RNAi}, *Apc* clones). At 10 days after induction, the cell proliferation and multilayering observed in N^{RNAi}, *Apc* clones was often extensive (Fig. 6A-D; see also Fig. S3 in the supplementary material), suggesting that *Apc* enhances the N^{RNAi} phenotype.

A quantitive analysis was performed to compare the number of ISCs generated in N^{RNAi}, *Apc* clones with the number of ISCs in marked N^{RNAi} lineages 5 days after induction (Fig. 6E-G; see also

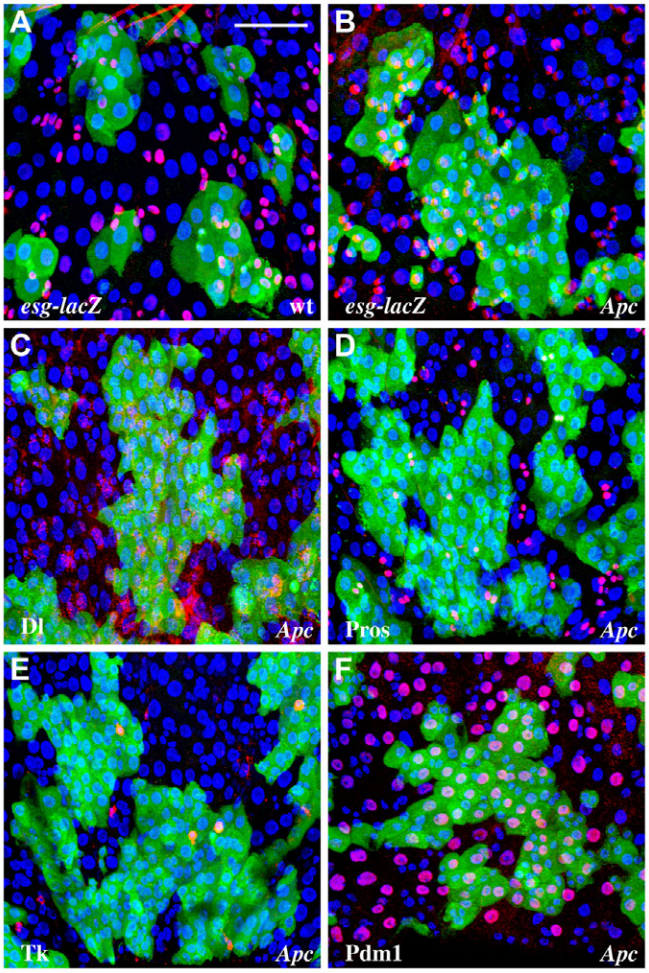

Fig. 5. Cell fate in the ISC lineage is correctly specified in the absence of *Apc*. (**A-F**) The MARCM system was used to positively identify ISC cell lineages with GFP 5 days after induction (anti-GFP, green; DAPI, blue). (A) Wild-type ISC lineages. *esg-lacZ* (red) marks the undifferentiated cells in the ISC lineage: stem cells and their undifferentiated EB daughters. (B) ISC lineages lacking *Apc*; *esg-lacZ* shown in red. Note the presence of both esg^+ and esg^- cells in marked *Apc* lineages. (C) ISC lineages lacking *Apc* (anti-Dl, red). (D) ISC lineages lacking *Apc*. Anti-pros (red) marks ee cells in the clone. (E) ISC lineages lacking *Apc*. Anti-Tachykinin (red) marks a subset of ee cells in the clone. (F) ISC lineages lacking *Apc*. Anti-Pdm1 (red) marks ECs. Scale bar: 50 μm.

Fig. S4A,B in the supplementary material). As in previous experiments, a 5-day time point was selected for this analysis to minimize the distortion of clone size due to multilayering. This comparison revealed a significant increase in the number of ISCs present in N^{RNAi}, *Apc* clones compared with in N^{RNAi} lineages alone (Fig. 6G; N^{RNAi}, *n*=116; N^{RNAi}, *Apc*, *n*=110; also compare with Fig. 4D for *Apc* alone). Thus, loss of *Apc* is sufficient to enhance the N^{RNAi} phenotype.

One explanation for the increased clone size in ISCs lacking both N^{RNAi} and *Apc* is that ISC proliferation has increased. If loss of *Apc* specifically affects stem cell proliferation, then we would expect to see an associated increase in the ISC mitotic index. Mitotic index was determined by counting the number of ISCs in M-phase as a function of the total number of ISCs (see Fig. S4C,D in the supplementary material). This analysis revealed a significant increase in the mitotic index of ISCs lacking both N and *Apc* compared with a lack of N alone (Fig. 6H; N^{RNAi}, *Apc*, *n*=16; N^{RNAi}, *n*=18). This finding, together with the increased size of N^{RNAi}, *Apc* mutant clones, demonstrates that the loss of *Apc* can affect ISC proliferation in the midgut independently of N-mediated cell fate specification.

Wnt signaling regulates homeostasis in ISC lineages

The requirement for Apc in the β-catenin destruction complex suggested that the Wnt signaling pathway might function to regulate the ISC lineage. To investigate this possibility, we first examined the effects of activating Wnt signaling on the size of marked ISC lineages. Wnt signaling was activated by generating mosaic animals expressing a constitutively active form of β-catenin, arm^{S10} (Pai et al., 1997). As in the case of *Apc* loss, arm^{S10} clones appeared abnormally large (see Fig. S5A-C in the supplementary material). To quantify the arm^{S10} phenotype, we compared the number of cells labeled in ISC lineages expressing arm^{S10} to the number in marked wild-type lineages 5 days after induction. This analysis revealed a significant effect of arm^{S10} on ISC clone size compared with wild-type controls (see Fig. S5D in the supplementary material). A comparison of the *Apc* and arm^{S10} phenotypes revealed that in both cases there was a significant increase in clone size relative to wild type. Nevertheless, the magnitude of the increase was greater following *Apc* loss than in the presence of arm^{S10}, as has been observed in other contexts (e.g. Pai et al., 1997; Hayden et al., 2007) (see Fig. S5D in the supplementary material). Thus, Wnt pathway activation leads to an increase in the size of marked ISC lineages.

Apc hyperplasia is suppressed by reductions in Wnt signaling

The finding that constitutive Wnt activation resembled *Apc* loss raised the possibility that hyperplasia observed in ISC lineages lacking *Apc* resulted from Wnt activation. To test this directly, we examined the effect of blocking Wnt signaling in *Apc* mutants. In these studies, Wnt signaling was reduced by generating mosaic animals expressing a dominant-negative form of *pangolin* (*pan*), $pan^{\Delta N}$, a transcription factor necessary for Wnt signaling (Brunner et al., 1997; van de Wetering et al., 1997). Control experiments showed first that, in contrast to wild-type lineages, mosaic expression of $pan^{\Delta N}$ resulted in reduced clone size 5 days after induction (Fig. 7A,B), as has previously been reported for the loss of other Wnt pathway components upstream of *pan* (Lin et al., 2008). Second, loss of a negative regulator in the Wnt pathway, *Axin* (Hamada et al., 1999b; Willert et al., 1999), phenocopied both *Apc* loss and arm^{S10} expression (Fig. 7C). Third, ISC lineages simultaneously expressing $pan^{\Delta N}$ and lacking *Axin* led to complete suppression of the *Axin* loss-of-function phenotype (Fig. 7D). Together, these control experiments established that $pan^{\Delta N}$ can suppress robust activation of the Wnt signaling pathway resulting from *Axin* loss. We next investigated whether $pan^{\Delta N}$ was sufficient to suppress the *Apc* double mutant phenotype. Simultaneous expression of $pan^{\Delta N}$ in ISC lineages lacking $Apc2^{33}$ and $Apc1^{Q8}$ led to a complete suppression of *Apc* hyperplasia (Fig. 7E,F). However, simultaneous expression of $pan^{\Delta N}$ in ISC lineages lacking $Apc2^{g10}$ and $Apc1^{Q8}$ resulted only in a partial suppression of the *Apc* phenotype (Fig. 7G,H). One potential explanation for these differences is that $Apc2^{g10}$, in contrast to $Apc2^{33}$, encodes a protein that retains an amino-terminal fragment, which has been shown to have an activating role in the Wnt signaling pathway (Takacs et al., 2008). Similarly truncated alleles of *Apc* are known to be associated with human adenomas (Lamlum et al., 1999; Rowan et al., 2000; Albuquerque et al., 2002; Cheadle et al., 2002). Taken

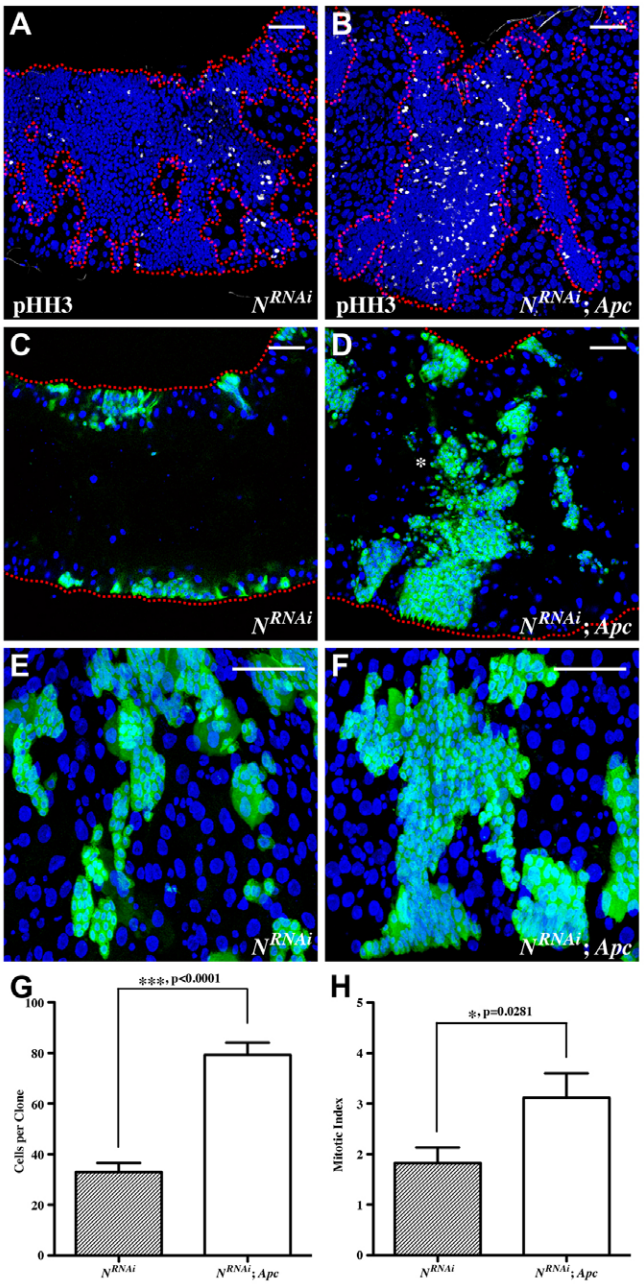

Fig. 6. *Apc* is required in ISCs to regulate proliferation. (**A-F**) The MARCM system was used to positively identify ISC lineages with GFP. (A,B) Clone outlines indicated in red, nuclei in blue (DAPI), and dividing cells in white (phospho-histone H3). (A) ISC clones expressing N^{RNAi} 10 days after induction. (B) ISC clones expressing N^{RNAi} and lacking *Apc*, 10 days after induction. (C,D) ISC lineages marked with GFP (anti-GFP, green; DAPI, blue); dashed red line indicates midgut outline. (C) ISC clones expressing N^{RNAi} 10 days after induction. (D) ISC clones expressing N^{RNAi} and lacking *Apc*, 10 days after induction. Extensive multilayering is evident in cross section. Asterisk indicates hyperplalastic cells in lower focal planes extending up into the luminal space. (E-H) Quantitation of ISC proliferation phenotype. (E) ISC clones expressing N^{RNAi} 5 days after induction. (F) ISC clones expressing N^{RNAi} and lacking *Apc*, 5 days after induction. (**G**) Comparison of N^{RNAi} and N^{RNAi}, *Apc* clone size 5 days after induction. N^{RNAi}, *Apc* loss leads to an increase in number of cells per clone (N^{RNAi}, n=116; N^{RNAi}, *Apc*, n=110). (**H**) Comparison of N^{RNAi} and N^{RNAi}, *Apc* mitotic index 5 days after induction. *Apc* loss leads to an increase in the ISC mitotic index (N^{RNAi}, n=18; N^{RNAi}, *Apc*, n =16). Error bars denote s.e.m. Scale bars: 50 μm.

together, our studies show that the abrogation of Wnt signaling in ISC lineages is sufficient to suppress the effect of *Apc* loss in an allele-specific manner.

DISCUSSION

In the current study, we report that loss of *Apc* results in a disruption of midgut homeostasis and is associated with hyperplasia and multilayering of the midgut epithelium. Our mosaic analyses show that *Apc* is required specifically in ISCs to regulate stem cell proliferation. By contrast, loss of *Apc* did not detectably affect self-renewal or cell fate specification in the ISC lineage. Activation of Wnt signaling in the ISC lineage phenocopied *Apc* loss and *Apc* mutants were suppressed in an allele-specific manner by abrogating Wnt signaling, suggesting that the effects of *Apc* are mediated in part by the Wnt pathway. The finding that *Apc* differentially affects ISC proliferation without obviously altering self-renewal or multipotency highlights the ability of the stem cell to fine-tune lineage output to meet homeostatic need; loss of *Apc* appears to short-circuit this regulation, providing increased cellular output in the absence of true physiological demand for new cells.

Previous analysis of Wnt signaling in the midgut has led to the assertion that Wnt functions as the primary maintenance signal for ISCs; cell-autonomous loss of Wnt transduction components results in a failure of ISC maintenance, while ectopic expression of Wnt ligand leads to an increase in the number of Dl-expressing cells (Lin et al., 2008). These observations led to the following model: transduction of the Wnt signaling pathway in ISCs adjacent to a Wnt source maintains the stem cell population by preventing lineage differentiation. A central prediction of the model is that cell-autonomous activation of the Wnt signaling pathway in ISCs should lead to the production of daughter cells, which constitutively transduce the Wnt signal and, as such, remain undifferentiated. The predicted consequence of this manipulation is an expansion in the number of ISCs at the expense of differentiated cells within the lineage, as has been observed in the case of *N* loss (Micchelli and Perrimon, 2006; Ohlstein and Spradling, 2006; Ohlstein and Spradling, 2007). In this study, we directly tested this prediction by analyzing marked ISC lineages. Our experiments clearly demonstrate that in contrast to *N* loss, ISCs lacking *Apc* generate both differentiated cell types of the adult midgut: ee cells and ECs. Importantly, these findings suggest that ISCs and their daughters are not distinguished solely on the basis of Wnt signal transduction.

Several explanations could account for these apparent disparities. First, it is worth noting that although Dl might be a reliable marker for certain stem cells in wild-type midguts, this might not be the case in every mutant background examined. For example, a previous analysis in *Drosophila* has demonstrated that Wnt activation is sufficient to stimulate high levels of Dl expression in a cell-autonomous manner (Micchelli et al., 1997). Thus, it is possible that Wnt pathway activation can uncouple Dl expression from stem cell identity, thereby diminishing the utility of Dl as a reliable stem cell marker. A second possible explanation is methodological; the use of genetic mosaic analyses to analyze individual ISC lineages, as in this study, might provide a different view of the Wnt pathway activation phenotype to that seen following the use of Gal4 driver lines. Third, it is possible that Wnt can affect stem cell maintenance upstream of *Apc* via a non-canonical pathway. For example, studies have demonstrated that Wnt signaling can act directly via *dishevelled* (*dsh*) to inhibit the N signaling pathway (Axelrod et al., 1996; Rulifson et al., 1996). Such effects might not be detected in the *Apc*, *Axin* or activated arm^{S10} ISC lineages analyzed here.

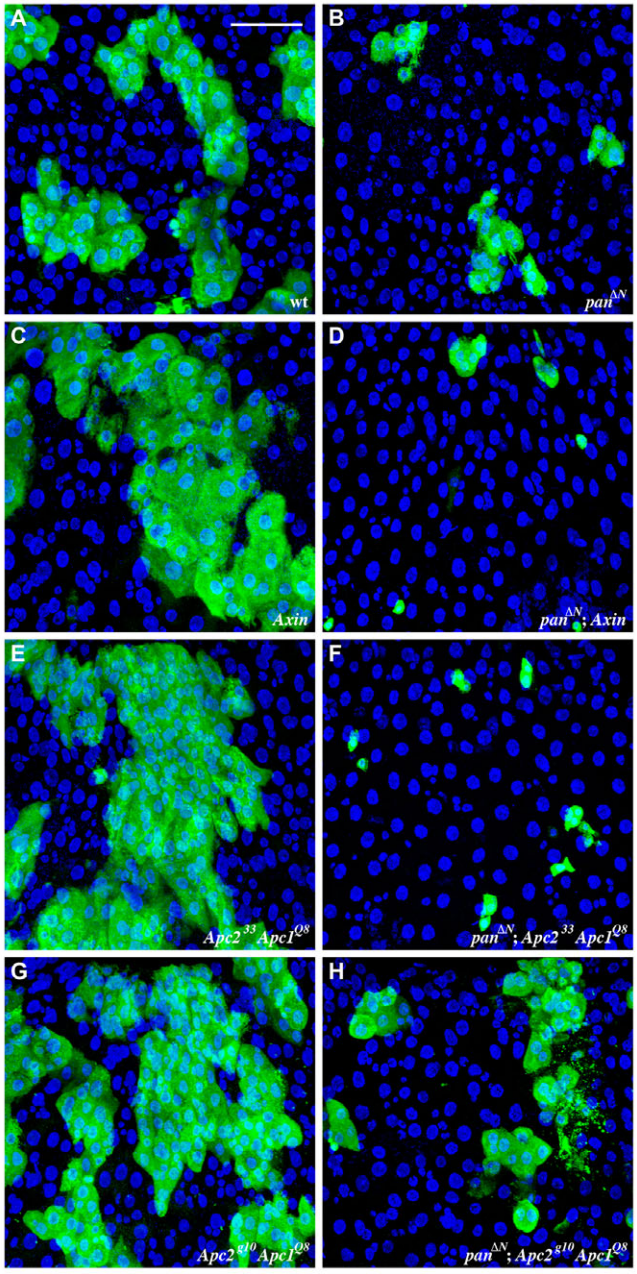

Fig. 7. *Apc* hyperplasia is suppressed by reducing Wnt signaling. (**A-H**) The MARCM system was used to positively identify posterior ISC cell lineages with GFP 5 days after induction (anti-GFP, green; DAPI, blue). (A) Wild-type ISC lineages. (B) ISC lineages expressing $pan^{\Delta N}$ (dominant negative). (C) ISC lineages lacking *Axin*. (D) ISC lineages lacking *Axin* and expressing $pan^{\Delta N}$. (E) ISC lineages lacking $Apc2^{33}$ and $Apc1^{Q8}$. (F) ISC lineages lacking $Apc2^{33}$ and $Apc1^{Q8}$, and expressing $pan^{\Delta N}$. Note that hyperplasia is suppressed. (G) ISC lineages lacking $Apc2^{g10}$ and $Apc1^{Q8}$. (H) ISC lineages lacking $Apc2^{g10}$ and $Apc1^{Q8}$, and expressing $pan^{\Delta N}$. Scale bar: 50 μm.

In this study, we have demonstrated an increase in the number of dividing cells following *Apc* loss, which is consistent with what has previously been reported for mutations that activate the Wnt pathway (Lin et al., 2008). And yet, as discussed above, the presence of differentiated cells within marked *Apc* mutant lineages strongly suggested that the increase in dividing cells could not be explained solely by a N-dependent change in cell fate within the ISC lineage as was proposed by Lin et al. Based on our analysis of *Apc*, we hypothesized that the increased proliferation following *Apc* loss reflects a cell-autonomous requirement for *Apc* specifically in ISCs. This view is further supported by the observation that *Apc* loss can lead to an increase in mitotic index when N and *Apc* are simultaneously removed from the ISC lineage. Thus, there is a requirement for *Apc* specifically in ISCs to regulate proliferation that is separable from N-dependent cell fate specification. Taken together, we conclude that a primary requirement for *Apc* in the ISC lineage is to autonomously restrict the proliferation of ISCs, and not to regulate the choice of cell fate.

On the basis of our findings we propose that ISC activity is regulated by the level of Wnt signal transduction (Fig. 8). In this model, Wnt functions as a permissive signal for ISC self-renewal, as we show that constitutive Wnt activation is not a sufficient criterion to convert all ISC progeny to stem cells, nor is activation sufficient to alter the fidelity of ISC self-renewal. Intermediate levels of Wnt define an adaptive homeostatic range, which permits the midgut to respond to environmental changes that the organism encounters. ISCs transducing Wnt at levels outside this range appear refractory to homeostatic input, as low levels of Wnt are associated with ISC loss, whereas Wnt activation leads to hyperplasia.

Nevertheless, our data do not rule out additional roles for *Apc* in the ISC lineage. For example, it is possible that the hyperplasia observed in *Apc* mutants reflects the combined requirement of *Apc* to regulate proliferation both in the ISCs and in nascent EB daughters. Similarly, *Apc* might also play a role in regulating cell turnover in the midgut. Indeed, several of our observations support the view that *Apc* might, in fact, be required for EC differentiation. First, mosaic analysis of *Apc* shows that cells of the lineage contribute to the multilayering phenotype, which suggests that mutant cells might have failed to properly establish appropriate adhesive contacts with the monolayer and/or the surrounding extracellular matrix (Fig. 3D,F). Second, although ECs lacking *Apc* appear to have large, polyploid nuclei and express molecular markers such as Pdm1, their nuclei are often detectably smaller than those of wild-type ECs (Fig. 4B,C). Furthermore, ECs lacking *Apc* often exhibit a restricted basal profile, failing to develop the tiled morphology that is characteristic of wild-type ECs (Fig. 4B,C). Finally, in the absence of *Apc*, ECs often display reduced cytoplasm, suggesting a requirement for cellular growth, a requirement that is not observed in either *Axin* mutant or arm^{S10}-expressing ICS lineages (Fig. 7; see also Fig. S5 in the supplementary material).

The discovery that *Apc* is somatically mutated in cells of the smallest human adenomas (Miyoshi et al., 1992; Powell et al., 1992) and that the frequency of *Apc* mutations detected among early adenomas is roughly the same as the frequency of *Apc* mutations in more advanced carcinomas (Powell et al., 1992) were among the seminal observations that established *Apc* as the rate-limiting step for gastrointestinal tumor initiation (reviewed by Kinzler and Vogelstein, 1996; Clevers, 2006). Subsequently, a number of *Apc* models have been established in both mouse and zebrafish to study gastrointestinal tumorigenesis (Su et al., 1992; Fodde et al., 1994; Oshima et al., 1995; Haramis et al., 2006). Yet, the precise cell(s) in which *Apc* is required remained unknown. Recently, through the use of refined genetic cell lineage tracing methodologies in the mouse, specific subpopulations of cells in the intestinal mucosa have been identified (e.g. $Lgr5^{+}$ and $Bmi1^{+}$), which display the ability to self-renew and undergo multilineage differentiation (Barker et al., 2007; Sangiorgi and Capecchi, 2008).

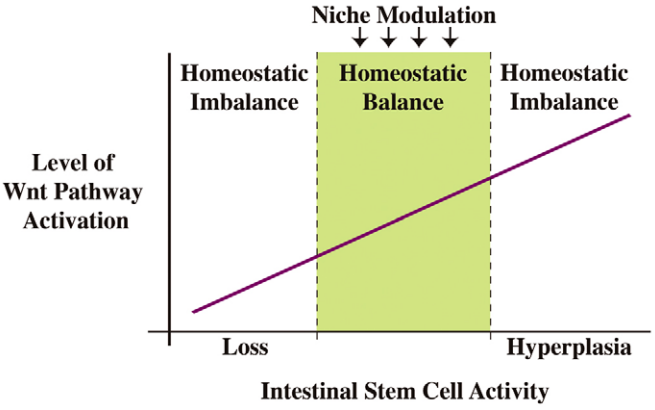

Fig. 8. Wnt regulation of midgut ISCs. Wnt functions as a permissive signal, and at intermediate levels of signal transduction defines an adaptive homeostatic range for ISCs activity (green). In this model, niche modulation fine-tunes ISC activity within this adaptive homeostatic range.

Subsequent studies have demonstrated that deletion of *Apc* specifically within the *Lgr5*$^{+}$ cell population leads to the formation of rapidly proliferating cells in both the large and small intestine (Barker et al., 2009). Thus, in the case of both *Drosophila* ISCs and mouse *Lgr5*$^{+}$ cells, loss of *Apc* leads to a disruption of homeostasis in the intestinal stem cell lineage. The remarkable parallels that exist between the dipteran and mammalian gastrointestinal tract suggest that the *Drosophila* midgut will continue to be a powerful genetic model system with which to dissect the molecular mechanisms underlying tumor initiation.

We thank B. McCarthy, Y. Ahmed and Bloomington Stock Center for generously providing *Drosophila* stocks; D. Nässel, W. Chia, X. Yang and Developmental Studies Hybridoma Bank for generously providing *Drosophila* antibodies. K.B. is an Olin Scholar. C.A.M. is a Pew Biomedical Research Scholar. This work was supported by development funds from Washington University School of Medicine, the Stem Cell Research Foundation, and the American Cancer Society.

Supplementary material

Supplementary material for this article is available at http://dev.biologists.org/cgi/content/full/136/13/2255/DC1

References

Ahmed, Y., Hayashi, S., Levine, A. and Wieschaus, E. (1998). Regulation of armadillo by a *Drosophila APC* inhibits apoptosis during retinal development. *Cell* **93**, 1171-1182.

Ahmed, Y., Nouri, A. and Wieschaus, E. (2002). *Drosophila Apc*1 and *Apc*2 regulate Wingless transduction throughout development. *Development* **129**, 1751-1762.

Akong, K., Grevengoed, E. E., Price, M. H., McCartney, B. M., Hayden, M. A., DeNofrio, J. C. and Peifer, M. (2002a). *Drosophila APC2* and *APC1* play overlapping roles in wingless signaling in the embryo and imaginal discs. *Dev. Biol.* **250**, 91-100.

Akong, K., McCartney, B. M. and Peifer, M. (2002b). *Drosophila APC*2 and *APC*1 have overlapping roles in the larval brain despite their distinct intracellular localizations. *Dev. Biol.* **250**, 71-90.

Albuquerque, C., Breukel, C., van der Luijt, R., Fidalgo, P., Lage, P., Slors, F. J. M., Leitao, C. N., Fodde, R. and Smits, R. (2002). The 'just-right' signalling model: APC somatic mutations are selected based on a specific level of activation of the β-catenin signalling cascade. *Hum. Mol. Genet.* **11**, 1549-1560.

Axelrod, J. D., Matsuno, K., Artavanas-Tsakonas, S. and Perrimon, N. (1996). Interaction between Wingless and Notch signaling pathways mediated by Dishevelled. *Science* **271**, 1826-1832.

Barker, N., van Es, J. H., Kuipers, J., Kujala, P., van den Born, M., Cozijnsen, M., Haegebarth, A., Korving, J., Begthel, H., Peters, P. J. et al. (2007). Identification of stem cells in small intestine and colon by marker gene Lgr5. *Nature* **449**, 1003-1007.

Barker, N., Ridgway, R. A., van Es, J. H., van de Wetering, M., Begthel, H., van den Born, M., Danenberg, E., Clarke, A. R., Sansom, O. J. and Clevers, H. (2009). Crypt stem cells as the cells-of-origin of intestinal cancer. *Nature* **457**, 608-611.

Brunner, E., Peter, O., Schweizer, L. and Basler, K. (1997). pangolin encodes a Lef-1 homolog that acts downstream of Armadillo to transduce the Wingless signal in Drosophila. *Nature* **385**, 829-833.

Cheadele, J. P., Krawczak, M., Thomas, M. W., Kodges, A. K., Al-Tassan, N., Pleming, N. and Sampson, J. R. (2002). Different combinations of biallelic APC mutation confer different growth advantages in colorectal tumors. *Cancer Res.* **62**, 363-366.

Clevers, H. (2006). Wnt/β-catenin signaling in development and disease. *Cell* **127**, 469-480.

Fodde, R., Edelmann, W., Yang, K., van Leeuwen, C., Carlson, C., Renault, B., Breukel, C., Alt, E., Lipkin, M., Khan, P. M. et al. (1994). A targeted chain termination mutation in the mouse *Apc* gene results in multiple intestinal tumors. *Proc. Natl. Acad. Sci. USA* **91**, 8969-8973.

Groden, J., Thliveris, A., Samowitz, W., Carlson, M., Gelbert, L., Albertsen, H., Joslyn, G., Stevens, J., Spirio, L. and Robertson, M. et al. (1991). Identification and characterization of the familial adenomatous polyposis coli gene. *Cell* **66**, 589-600.

Hamada, F., Murata, Y., Nishida, A., Fujita, F., Tomoyasu, Y., Nakamura, M., Toyoshima, K., Tabata, T., Ueno, N. and Akiyama, T. (1999a). Identification and characterization of E-*APC*, a novel *Drosophila* homologue of the tumor suppressor *APC*. *Genes Cells* **4**, 465-474.

Hamada, F., Tomoyasu, Y., Takatsu, Y., Nakamura, M., Nagai, S., Suzuki, A., Fujita, F., Shibuya, H., Toyoshima, K., Ueno, N. et al. (1999b). Negative regulation of Wingless signalling by D-Axin, a *Drosophila* homolog of Axin. *Science* **283**, 1739-1942.

Haramis, A. P., Hurlstone, A., van der Velden, Y., Begthel, H., van den Born, M., Offerhaus, G. J. and Clevers, H. C. (2006). Adenomatous polyposis coli-deficient zebrafish are susceptible to digestive tract neoplasia. *EMBO Rep.* **7**, 444-449.

Hayashi, S., Rubinfeld, B., Souza, B., Polakis, P., Wieschaus, E. and Levine, A. J. (1997). A *Drosophila* homolog of the tumor suppressor gene *adenomatous polyposis coli* down-regulates β-catenin but its zygotic expression is not essential for the regulation of Armadillo. *Proc. Natl. Acad. Sci. USA* **94**, 242-247.

Hayden, M. A., Akong, K. and Peifer, M. (2007). Novel roles for *APC* family members and Wingless/Wnt signaling during *Drosophila* brain development. *Dev. Biol.* **305**, 358-376.

Ichii, S., Horii, A., Nakatsuru, S., Furuyama, J., Utsunomiya, J. and Nakamura, Y. (1992). Inactivaton of both *APC* alleles in an early stage of colon adenoma in a patient with familial adenomatous polyposis (FAP). *Hum. Mol. Genet.* **1**, 387-390.

Jones, D. L. and Wagers, A. J. (2008). No place like home: anatomy and function of the stem cell niche. *Nat. Rev.* **9**, 11-21.

Kinzler, K. W. and Vogelstein, B. (1996). Lessons from hereditary colorectal cancer. *Cell* **87**, 159-170.

Kinzler, K. W., Nilbert, M. C., Su, L. K., Vogelstein, B., Bryan, T. M., Levy, D. B., Smith, K. J., Preisinger, A. C., Hedge, P., McKechnie, D. et al. (1991). Identification of FAP locus genes from chromosome 5q21. *Science* **253**, 661-665.

Lamlum, H., Ilyas, M., Rowan, A., Clark, S., Johnson, V., Bell, J., Frayling, I., Efstathiou, J., Pack, K., Payne, S. et al. (1999). The type of somatic mutation at APC in familial adenomatous polyposis is determined by the site of the germline mutation: a new facet to Knudson's 'two-hit' hypothesis. *Nat. Med.* **5**, 1071-1075.

Lee, T. and Luo, L. (1999). Mosaic analysis with a repressible cell marker for studies of gene function in neural morphogenesis. *Neuron* **22**, 451-461.

Lin, G., Xu, N. and Xi, R. (2008). Paracrine Wingless signaling controls self-renewal of *Drosophila* intestinal stem cells. *Nature* **455**, 310-312.

Margolis, J. and Spradling, A. (1995). Identification and behavior of epithelial stem cells in the *Drosophila* ovary. *Development* **121**, 3797-3807.

McCartney, B. M., Dierick, H. A., Kirkpatrick, C., Moline, M. M., Baas, A., Peifer, M. and Bejsovec, A. (1999). *Drosophila APC*2 Is a cytoskeletally-associated protein that regulates Wingless signaling in the embryonic epidermis. *J. Cell Biol.* **146**, 1303-1318.

McCartney, B. M., Price, M. H., Webb, R. L., Hayden, M. A., Holot, L. M., Zhou, M., Bejsovec, A. and Peifer, M. (2006). Testing hypothesis for the functions of *APC* family proteins using null and truncation alleles in *Drosophila*. *Development* **133**, 2407-2418.

Micchelli, C. A. and Perrimon, N. (2006). Evidence that stem cells reside in the adult *Drosophila* midgut epithelium. *Nature* **439**, 475-479.

Micchelli, C. A., Rulifson, E. J. and Blair, S. S. (1997). The function and regulation of cut on the wing margin of *Drosophila:* Notch, Wingless and a dominant negative role for Delta and Serrate. *Development* **124**, 1485-1495.

Miller, A. (1950). The internal anatomy and histology of the imago of Drosophila melanogaster. In *Biology of Drosophila* (ed. M. Demerec), pp. 420-534. New York: John Wiley.

Miyoshi, Y., Nagase, H., Ando, H., Horii, A., Ichii, S., Nakatsuru, S., Aoki, T., Miki, Y., Mori, T. and Makamura, Y. (1992). Somatic mutations of the *APC* gene in colorectal tumors: mutation cluster region in the *APC* gene. *Hum. Mol. Genet.* **1**, 229-233.
Morrison, S. J. and Spradling, A. C. (2008). Stem cells and niches: mechanisms that promote stem cell maintenance throughout life. *Cell* **132**, 598-611.
Ohlstein, B. and Spradling, A. (2006). The adult *Drosophila* posterior midgut is maintained by pluripotent stem cells. *Nature* **439**, 470-474.
Ohlstein, B. and Spradling, A. (2007). Multipotent *Drosophila* intestinal stem cells specify daughter cell fates by differential notch signaling. *Science* **315**, 988-992.
Oshima, M., Oshima, H., Kitagawa, K., Kobayashi, M., Itakura, C. and Taketo, M. (1995). Loss of *Apc* heterozygosity and abnormal tissue building in nascent intestinal polyps in mice carrying a truncated *Apc* gene. *Proc. Natl. Acad. Sci. USA* **92**, 4482-4486.
Pai, L. M., Orsulic, S., Bejsovec, A. and Peifer, M. (1997). Negative regulation of Armadillo, a Wingless effector in *Drosophila*. *Development* **124**, 2255-2266.
Powell, S. M., Zilz, N., Beazer-Barclay, Y., Bryan, T. M., Hamilton, S. R., Thibodeau, S. N., Vogelstein, B. and Kinzler, K. W. (1992). *APC* mutations occur early during colorectal tumorigenesis. *Nature* **359**, 235-237.
Presente, A., Shaw, S., Nye, J. S. and Andres, A. J. (2002). Transgene-mediated RNA interference defines a novel role for Notch in chemosensory startle behavior. *Genesis* **34**, 165-169.
Rowan, A. J., Lamlum, H., Ilyas, M., Wheeler, J., Straub, J., Papadopoulou, A., Bicknell, D., Bodmer, W. F. and Tomlinson, I. P. (2000). APC mutations in sporadic colorectal tumors: a mutational 'hotspot' and interdependence of the 'two hits'. *Proc. Natl. Acad. Sci. USA* **97**, 3352-3357.
Rubinfeld, B., Albert, I., Porfiri, E., Munemitsu, S. and Polakis, P. (1997). Loss of beta-catenin regulation by the *APC* tumor suppressor protein correlates with loss of structure due to common somatic mutations of the gene. *Cancer Res.* **57**, 4624-4630.
Rulifson, E. J., Micchelli, C. A., Axelrod, J. D., Perrimon, N. and Blair, S. S. (1996). wingless refines its own expression domain on the *Drosophila* wing margin. *Nature* **384**, 72-74.
Sangiorgi, E. and Capecchi, M. R. (2008). *Bmi1* is expressed *in vivo* in intestinal stem cells. *Nat. Genet.* **40**, 915-920.
Siviter, R. J., Coast, G. M., Winther, A. M., Nachman, R. J., Taylor, C. A., Shirras, A. D., Coates, D., Isaac, R. E. and Nässel, D. R. (2000). Expression and functional characterization of a *Drosophila* neuropeptide precursor with homology to mammalian preprotachykinin A. *J. Biol. Chem.* **275**, 23273-23280.
Su, L. K., Kinzler, K. W. and Vogelstein, B., Preisinger, A. C., Moser, A. R., Luongo, C., Gould, K. A. and Dove, W. F. (1992). Multiple intestinal neoplasia caused by a mutation in the murine homolog of the *APC* gene. *Science* **256**, 668-670.
Su, L. K., Vogelstein, B. and Kinzler, K. W. (1993). Association of the APC tumor suppressor protein with catenins. *Science* **262**, 1734-1737.
Takacs, C. M., Baird, J. R., Hughes, E. G., Kent, S. S., Benchabane, H., Paik, R. and Ahmed, Y. (2008). Dual positive and negative regulation of wingless signaling by adenomatous polyposis coli. *Science* **319**, 333-336.
van de Wetering, M., Cavallo, R., Dooijes, D., van Beest, M., van Es, J., Loureiro, J., Ypma, A., Hursh, D., Jones, T., Bejovec, A. et al. (1997). Armadillo coactivates transcription driven by the product of the Drosophila segment polarity gene dTCF. *Cell* **88**, 789-799.
Willert, K., Logan, C. Y., Arora, A., Fish, M. and Nusse, R. (1999). A *Drosophila Axin* homolog, *Daxin*, inhibits Wnt signaling. *Development* **126**, 4165-4173.
Yeo, S. L., Lloyd, A., Kozak. K., Dinh, A., Dick, T., Yang, X., Sakonju, S. and Chia, W. (1995). On the functional overlap between two *Drosophila* POU homeo domain genes and the cell fate specification of a CNS neural precursor. *Genes Dev.* **15**, 1223-1236.